EFFECT OF VOLUME FRACTION AND INTERFACIAL AREA BETWEEN FIBRE AND RESIN ON MECHANICAL PROPERTIES OF CNF-ADDED NATURAL FIBRE REINFORCED PLA COMPOSITES

SEIJI MITSUBAYASHI & KENICHI TAKEMURA
Department of Mechanical Engineering, Kanagawa University, Japan

ABSTRACT

In recent years, green composites (GCs), which are biodegradable resins reinforced with natural fibres and have excellent specific strength, have attracted attention from the viewpoint of environmental impact. To improve the mechanical properties of GCs, it is necessary to enhance the interfacial adhesion between fibre and resin, and recent attempts have been focused on improving the mechanical properties of GCs by adding cellulose nanofibres (CNF) to the interface between fibre and resin. However, the effects of volume fraction and interfacial area between fibre and resin on the mechanical properties of CNF-added natural fibre reinforced composites have not been clarified. Therefore, to explain these effects, the tensile strength of CNF-added natural fibre reinforced composites was evaluated by varying the content of twisted natural fibres in the composites and the interfacial area between the fibres and the resin. The following conclusions can be obtained from this study: (1) The tensile strength of natural fibre-reinforced PLA composites decreases as the interfacial area between the fibres and the resin increases, even when the fibre volume is the same; and (2) Although the tensile strength can be improved by increasing the amount of CNF as the interfacial area increases, the strength cannot be improved as much as when the interfacial area is small because the fibres tend to aggregate.

Keywords: green composites, natural fibre, volume fraction, interfacial area, cellulose nanofibre, tensile strength.

1 INTRODUCTION

In recent years, green composites (GCs) have been developed to reduce environmental impact. GCs are composites that use biodegradable resin as the matrix and natural fibres as reinforcement. They have attracted attention from a sustainability perspective [1]–[3]. However, GCs have inferior mechanical properties compared to carbon fibre reinforced plastics (CFRP) and glass fibre reinforced plastics (GFRP) [4], [5].

The main reasons for the lower mechanical properties of GCs are (1) low adhesion at the fibre/resin interface, (2) heterogeneous fibre dispersion, and (3) degradation due to the hygroscopic properties of natural fibres [6], [7]. In particular, low interfacial adhesion causes fibre pullout and interface debonding under tensile loading, resulting in a decrease in mechanical strength [8]. Therefore, it is necessary to reduce the area of the fibre/resin interface when designing GC.

On the other hand, in practice, there are cases where the interface area needs to be increased. For example, when the fibre content is increased to increase the percentage of reinforcement and the overall strength [9], an increase in the interfacial area is inevitable. The interfacial area also needs to be increased when there is a limit to the fibre diameter when moulding GC. Therefore, if the area of the fibre/resin interface needs to be increased, appropriate interfacial strengthening techniques are essential.

Chemical surface modification techniques such as alkali treatment [10] and silane coupling treatment [11] have been proposed as methods to improve interfacial adhesion. Silane coupling treatment is a technique that improves interfacial adhesion by forming strong

WIT Transactions on The Built Environment, Vol 216, © 2025 WIT Press
www.witpress.com, ISSN 1743-3509 (on-line)
doi:10.2495/HPSM250071

chemical bonds between materials using silane compounds. Alkali treatment is a method of removing lignin and hemicellulose from the fibre surface using alkaline chemicals such as sodium hydroxide. However, these chemical treatments are costly and have a large environmental impact [12]. Therefore, there is a need for an interface strengthening method with a lower environmental burden.

In recent years, the reinforcement of interfaces using cellulose nanofibres (CNF) has gained attention. CNF is a naturally derived material with a nanoscale high specific surface area and low environmental impact [13]. It is expected to function as a nanoscale reinforcing agent, enhancing the mechanical strength of the interface [14], [15]. Therefore, to mitigate the deterioration of mechanical properties caused by increased interfacial area and to ensure stable strength characteristics, CNF-based interfacial reinforcement is considered effective. However, the effect of CNF addition on the mechanical properties of natural fibre-reinforced PLA composites is assumed to change depending on fibre volume fraction and fibre/matrix interfacial area. The influence of these parameters on the mechanical properties of CNF-reinforced natural fibre/PLA composites has not yet been fully clarified.

Therefore, in this study, multiple specimens were prepared with varying fibre volume fractions and fibre/matrix interfacial areas to investigate their effects on the mechanical properties of natural fibre-reinforced PLA composites. Furthermore, CNF was added at different concentrations to specimens with modified interfacial areas, and the changes of interfacial adhesion were compared.

2 EXPERIMENTAL METHOD

2.1 Materials

In this study, four types of twisted ramie yarns were used as reinforcing materials. Among them, the 7, 20, and 60 count twisted yarns were all obtained from Tosco Co., Ltd. and Tokyo, Japan, while only the 40 count was obtained from Bookbinding Studio Marumizu-Gumi, Tokyo, Japan. In this context, the term ‘count’ refers to the metric count (Nm), which can be converted to tex, the mass per kilometre of twisted yarn, using eqn (1):

$$\text{tex} = \frac{1000}{\text{Nm}}, \tag{1}$$

where tex and Nm are the linear density in tex and the metric count, respectively.

Polylactic acid (PLA) (TERRAMAC TE-2000, UNITIKA Ltd., Osaka, Japan) was used as the base material, which had a specific gravity of 1.25, a melting temperature of 170°C, and a melt flow rate of 10 g/10 min (190°C, 21.18 N) [16].

Additionally, CNF (BiNFi-s, WFo-10002, Sugino Machine Co. Ltd., Japan) was used as an additive. The CNF used in this study is commercially available in slurry form, dissolved at a concentration of 2 wt. To incorporate CNF into the ramie twisted yarns, the CNF slurry was first diluted with distilled water and then stirred using a homogenizer.

2.2 Fabrication process of specimens

2.2.1 Fabrication process of CNF-added ramie yarn reinforced PLA composites

Fig. 1 shows the apparatus for producing ramie twisted yarn reinforced PLA filament. Alkali treatment and compositing with PLA were performed using this apparatus while feeding twisted yarns at a constant speed. The twisted yarns were unwound for transport (part no. 1 in Fig. 1) and the rollers were rotated while nipping the twisted yarns (part no. 2). A motor

was attached to each roller, and the twisted yarns were conveyed by adjusting the rotation speed of each roller. Here, the twisted yarns were conveyed while making sure that tension was applied to the twisted yarns so that they would not sag (part no. 3). When adding CNF to the conveyed twisted yarns, CNF was adhered to the ramie twisted yarns while feeding CNF slurry into a container (part no. 4) using a roller tube pump. Here, the CNF was agitated beforehand in a process homogenizer to fully agitate the CNF in the slurry. The rotational speed and operation time of the homogenizer during agitation were set to 2500 rpm and 30 minutes, respectively. In this study, to inhibit hydrolysis of PLA resin, twisted yarns with CNF were thoroughly dried in a vacuum dryer. Here, the temperature and time for drying were 130°C and 4 hours, respectively. After drying, the CNF-added ramie twisted yarns were conveyed into the crosshead die (part no. 7) and composited with PLA supplied by a single-shaft extruder (part no. 8). The composited ramie twisted yarn reinforced PLA composite was air cooled and finally wound while using a winding device (part no. 9).

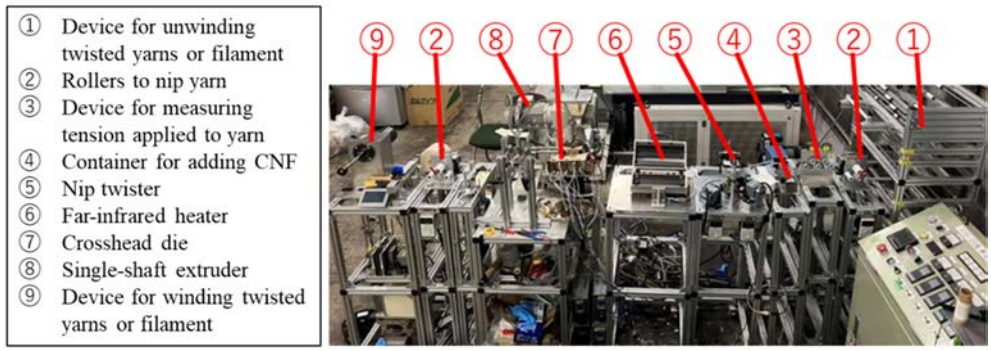

Figure 1: Equipment for the fabrication of CNF-added ramie yarn and ramie yarn reinforced composites.

2.2.2 Fabrication process of ramie yarn reinforced PLA composites

CNF-added ramie/PLA composites (filaments) were fabricated using the filament fabrication equipment shown in Fig. 1. The filament fabrication conditions are shown in Table 1 and Table 2. The filaments were fabricated while adjusting the diameter of the fabricated filaments to 1.6 mm. The filaments were also fabricated while adjusting the mass of CNF to be added in each condition in Table 2 between 0% and 1% of the mass of the slurry at 0.25% intervals. Here, when adding CNF, each twisted yarn was immersed in the slurry individually rather than immersing multiple yarns simultaneously.

Table 1: Fabrication conditions of filaments to evaluate the relationship between tensile strength and volume fraction of filaments.

No.	Count (Nm)	Number of yarns	Volume fraction (%)	CNF additive ratio (wt.%)
1	7	1	11.6	0
2	20	1	4.42	0
3	40	1	2.25	0
4	60	1	1.46	0

Table 2: Fabrication conditions of filaments for evaluating the relationship between tensile strength and fibre-resin interfacial area.

No.	Count (Nm)	Number of yarns	Volume fraction (%)	CNF additive ratio (wt.%)
1	20	1	4.42	0, 0.25, 0.50, 0.75, 1.0
2	40	2	4.50	0, 0.25, 0.50, 0.75, 1.0
3	60	3	4.38	0, 0.25, 0.50, 0.75, 1.0

2.3 Evaluation method of tensile properties

2.3.1 Tensile test of ramie yarn

In this study, the four types of ramie yarns shown in Table 1 were glued to a U-shaped backing paper with a 10 mm distance between the points, and the backing paper was then cut with scissors to prepare the test specimens. The test specimens were mounted on a universal testing machine (Tensilon, RTC-1250A, A&D Company, Limited, Tokyo, Japan) and static tensile tests were conducted. The number of specimens was set to 10 or more, and the tensile speed of the specimens was set to 1.0 mm/min.

When calculating the cross-sectional area, the shape of the twisted yarn was considered to be elliptical because of the flattened shape of the fibre. When measuring dimensions, the diameters of the major and minor axes were measured by image analysis. Eqn (2) was used to calculate the cross-sectional area.

$$A = \frac{\pi ab}{4}, \tag{2}$$

where A, a, and b are the cross-sectional area, diameter of the major axis, and diameter of the minor axis of the twisted yarn, respectively.

2.3.2 Tensile test of ramie yarn reinforced PLA composites

Static tensile tests of ramie/PLA composites in filament shape were performed under each of the conditions listed in Table 1 and Table 2. Here, the length of the specimen was 150 mm, the distance between the points was 50 mm, the number of tests was 5, and the tensile speed of the specimen was 1.0 mm/min. A micrometre was used to measure the diameter.

2.4 Observation of fracture surface of ramie yarn reinforced PLA composite

A scanning electron microscope (SEM) (SU8010, Hitachi, Limited, Tokyo, Japan) was used to observe the fracture surface of the filaments. The acceleration voltage was set to 5.0 kV and the magnification to 250x to observe the shape of the fracture surface and voids. To observe the interface between the twisted yarns and resin, the acceleration voltage was set to 5.0 kV and the magnification was 500x.

3 RESULTS AND DISCUSSION

3.1 Tensile strength of ramie yarns

Fig. 2 shows the average tensile strength of 7-count, 20-count, 40-count, and 60-count ramie yarns, each measured five times. The values ranged from 235 to 260 MPa, with an average of approximately 250 MPa. Since all three yarn types exhibited similar strength, they can be considered equivalent regardless of yarn thickness.

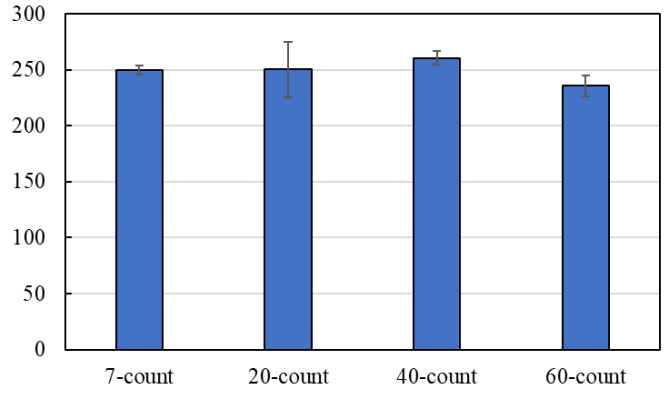

Figure 2: Tensile strength of ramie yarns.

3.2 Tensile strength of ramie yarn reinforced PLA composites

Fig. 3 shows a comparison between the tensile strength of filaments containing a single fibre for each of the 7, 20, 40, and 60 count yarns, as listed in Table 1, and the theoretical values calculated based on the rule of mixtures.

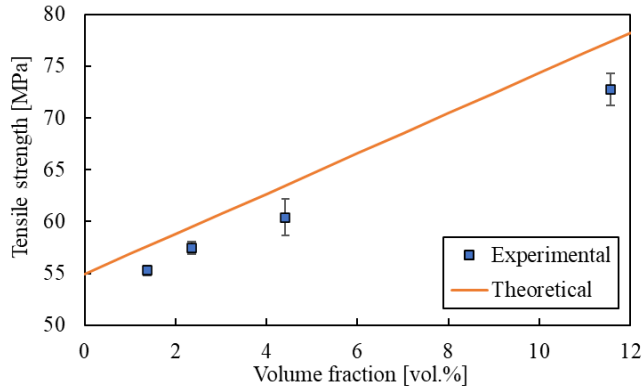

Figure 3: Relationship between tensile strength of ramie yarn reinforced PLA composites and volume fraction of yarn.

When applying the rule of mixtures, the load was assumed to act in the fibre direction. Therefore, the tensile strength of the FRP was determined as the volume-weighted average of the fibre and resin strengths, expressed as follows:

$$\sigma_c = \sigma_f V_f + \sigma_m V_m, \tag{3}$$

where σ represents the tensile strength, V denotes the volume fraction, and the subscripts c, m, and f refer to the composite, matrix, and fibre (yarn), respectively.

As shown in Fig. 3, the experimental values tended to be lower than the theoretical values calculated using the rule of mixtures. The failure of FRP can be attributed to multiple factors,

including fibre fracture, matrix failure, and interfacial debonding, which indicate that the actual strength does not always align with idealized theoretical predictions. Nevertheless, the results suggest the need for improvements in the tensile strength of the filament.

3.3 Effect of adding CNF on tensile strength of ramie yarn reinforced PLA filament

Fig. 4 presents the tensile strength of filaments fabricated under three different conditions: one 20-count yarn, two 40-count yarns, and three 60-count yarns. In these specimens, the volume fraction of ramie yarn was adjusted to approximately 4.4%, allowing for a comparison of the relationship between interfacial area and tensile strength. Additionally, the figure also illustrates the changes of tensile strength resulting from CNF addition. As figure 4 shows, it was observed that even with CNF addition, the maximum tensile strength was obtained under the one 20-count yarn condition. A comparison of the increase in tensile strength between 0 wt.% and 0.25 wt.% CNF addition showed that the highest increase was observed in the three count-60 yarns condition, followed by the two count-40 yarns and one count-20 yarn conditions. In particular, the condition with three 60-count yarns showed the greatest improvement in tensile strength. This is likely because it had the largest interfacial area, making it more responsive to the effects of CNF. However, at a CNF slurry concentration of 0.50 wt.%, a decrease in tensile strength was observed only in the condition with three 60-count yarns. This may be attributed to excessive CNF addition, leading to aggregation and a loss of interfacial uniformity.

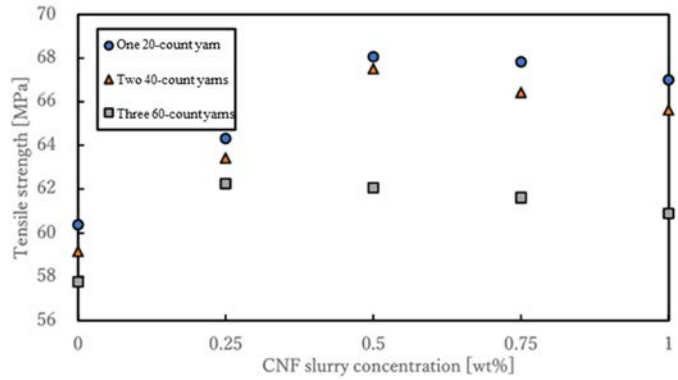

Figure 4: Relationship between tensile strength and CNF slurry concentration.

Furthermore, theoretical values were calculated using eqn (2) based on the rule of mixtures presented in Section 3.2, yielding a theoretical tensile strength of 63.5 MPa. A comparison between this theoretical value and the maximum tensile strength of the filaments under each condition was conducted to analyse the effect of CNF addition. As a result, under the conditions of using one 20-count yarn and two 40-count yarns, the measured tensile strength exceeded the theoretical value. In contrast, the measured tensile strength was lower than the theoretical value when using three 60-count yarns.

Scanning electron microscope (SEM) was used to observe the fracture surfaces of each filament. The observation results are shown in Fig. 5. In this figure, (a), (b), and (c) represent the fracture surfaces of the specimens obtained when 0.75 wt.% CNF slurry was added to 20-

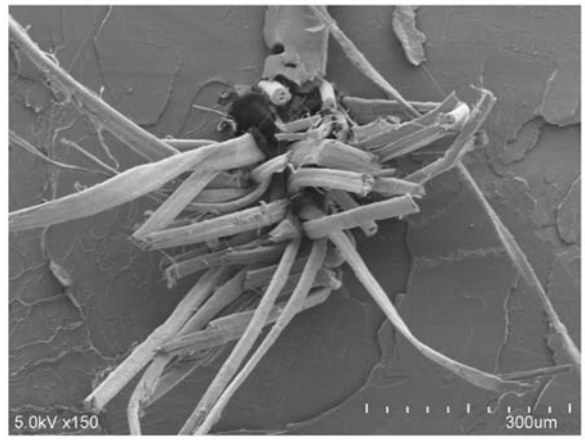

(a)

(b)

(c)

Figure 5: SEM images of ramie yarn reinforced PLA Filaments. (a) One 20-count yarn; (b) Two 40-count yarns; and (c) Three 60-count yarns.

count ramie twisted yarn, 0.75 wt.% CNF slurry was added to 40-count ramie twisted yarns, and 0.50 wt.% CNF slurry was added to 60-count ramie twisted yarns, respectively. As seen in Fig. 5(c), the weak interfacial adhesion likely caused fibre pull-out, resulting in a decrease in tensile strength. Similarly, Figs 5(a) and (b) show that weak interfacial adhesion led to fibre pull-out and a corresponding decrease in tensile strength.

3.4 Relationship between tensile strength and CNF content per unit length of CNF-added ramie yarn reinforced PLA composites

Fig. 6 shows the relationship between the tensile strength of filaments and the amount of added CNF. The filaments were produced under three conditions: one 20-count yarn, two 40-count yarns, and three 60-count yarns. The *x*-axis in Fig. 6 represents the CNF content per unit length of the filament. As shown in the Fig. 6, while the CNF content per strand decreases as the yarn diameter decreases, the CNF content per unit length of the filament tends to increase with a higher yarn count and an increased number of strands. Furthermore, when CNF was added to the 20-count yarn, a nearly proportional relationship between the CNF addition rate and the adhered amount was observed up to a CNF slurry concentration of 0.50 wt.%. However, beyond 0.50 wt.%, the adhesion ratio of CNF tended to decrease. Similarly, for both the 40-count and 60-count yarns, an increase in the CNF content resulted in a decrease in the adhesion ratio. By comparing these results with the tensile strength of the filaments, it was suggested that the decrease in filament strength was primarily due to CNF aggregation.

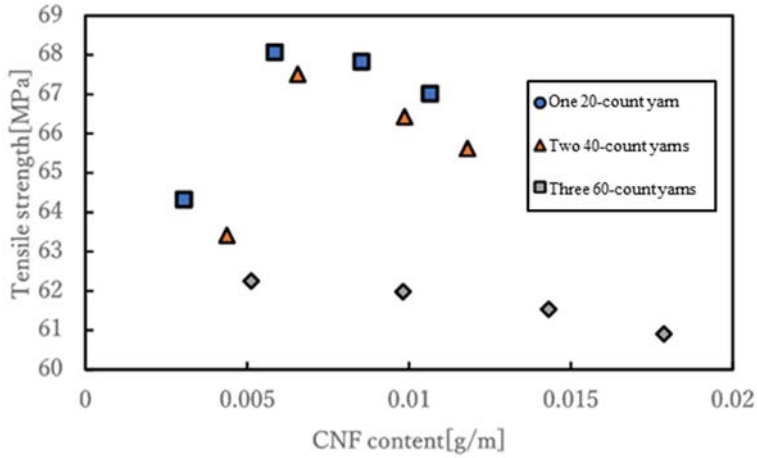

Figure 6: Relationship between tensile strength and CNF content.

When comparing the cross-sectional area per unit length of each twisted yarn, the cross-sectional areas of the 40-count and 60-count yarns are 1/2 and 1/3, respectively, of that of the 20-count yarn. Consequently, the diameters of the 40-count and 60-count yarns are $1/\sqrt{2}$ and $1/\sqrt{3}$, respectively. Thus, when comparing individual yarns, the interfacial surface area between the yarn and the resin follows the same ratio, with the 40-count and 60-count yarns having $1/\sqrt{2}$ and $1/\sqrt{3}$ of the interfacial area of the 20-count yarn. However, when considering the total interfacial area per unit length of the filament, the presence of two 40-

count yarns and three 60-count yarns results in an interfacial area that is $\sqrt{2}$ and $\sqrt{3}$ times that of a filament containing a single 20-count yarn, respectively. Although an increase in the interfacial bonding area between the yarn and the resin was expected to enhance interfacial reinforcement by CNF, in reality, the reduction in the interfacial bonding area per individual yarn led to increased CNF aggregation, which in turn contributed to a decrease in tensile strength.

4 CONCLUSION

In this study, tensile tests were conducted on composite materials to evaluate changes in tensile strength due to differences in the volume fraction of ramie yarn in the filaments and changes in tensile strength when the number of fibres was changed while maintaining the same volume fraction of ramie yarn in the filaments. The same evaluation was also conducted when CNF was added. The following are the findings obtained from these evaluations.

1. As the volume fraction of ramie twisted yarn in the filament increases, the tensile strength of the filament improves. Additionally, the tensile strength of each filament without CNF addition falls below the theoretical values calculated based on the rule of mixtures.
2. When the volume fraction of ramie twisted yarn in the filament is constant, a decrease in the yarn diameter leads to a reduction in tensile strength. This tendency is independent of CNF addition. Therefore, increasing the yarn diameter within the filament is necessary.
3. The addition of CNF enhances the tensile strength of filaments made with 20-count and 40-count twisted yarns, exceeding the theoretical values calculated based on the rule of mixtures. In contrast, for filaments produced using 60-count twisted yarn, the tensile strength does not surpass the theoretical values, even with CNF addition.
4. When the concentration of CNF slurry is 0.25 wt.% or lower, the tensile strength of the filament increases at a higher rate as the diameter of the twisted yarn decreases. This is because reducing the yarn diameter increases the interfacial area between the yarn and the resin, enhancing the tensile strength. However, when the CNF slurry concentration exceeds 0.25 wt.%, specimens with smaller yarn diameters tend to exhibit a lower rate of tensile strength improvement. This is likely due to the increased tendency of CNF aggregation.
5. The tensile strength of the filament depends not on the total interfacial area between the twisted yarn and resin but on the interfacial area per individual yarn. A decrease in the adhesion area at the yarn/resin interface for each yarn increases the likelihood of CNF aggregation, which contributes to this effect.

ACKNOWLEDGEMENTS

Some equipment was used in this study at the Research Institute for Engineering at Kanagawa University. We gratefully thank Mr. Miyase at Kanagawa University for his support in data acquisition.

REFERENCES

[1] Abdul Khalil, H.P.S., Bhat, A.H. & Ireana Yusra, A.F., Green composites from sustainable cellulose nanofibrils: A review. *Carbohydrate Polymers*, **87**(2), pp. 963–979, 2012.

[2] Dejene, B.K. & Geletaw, T.M., Development of fully green composites utilizing thermoplastic starch and cellulosic fibers from agro-waste: A critical review. *Polymer-Plastics Technology and Materials*, **63**(5), pp. 540–569, 2024.

[3] Somasundaram, R., Somasundaram, M., Ananchaperumal, P., Suyambulingam, I. & Siengchin, S., Enhancing properties and sustainability: Surface modified cymbopogon flexuosus stem fiber for green composite materials. *Polymer Composites*, **45**(3), pp. 2809–2824, 2024.
[4] Liu, J.L., Pham, V.N.H., Mencattelli, L., Chew, E., Chua, P.Y., Shen, J., Tian, K., Zhi, J., Jiang, D., Tay, T.E. & Tan, V.B.C., Improving the impact performance of natural fiber reinforced laminate through hybridization and layup design. *Composites Science and Technology*, **251**(26), 110585, 2024.
[5] Savas, S., Bakir, D. & Akcaat, Y.K., Experimental and numerical investigation of the usability of nonwoven hemp as a reinforcement material. *Case Studies in Construction Materials*, **20**, e03091, 2024.
[6] Singh, A.P., Zafar, S., Suman, S. & Pathak, H., Mechanical and electromagnetic interference shielding properties of natural fiber reinforced polymer composite with carbon nanotubes addition. *Polymer Composites*, **45**(5), pp. 4487–4501, 2024.
[7] Teeraphantuvat, T., Jatuwong, K., Jinanukul, P., Thamjaree, W., Lumyong, S. & Aiduang, W., Improving the physical and mechanical properties of mycelium-based green composites using paper waste. *Polymers*, **16**(2), p. 262, 2024.
[8] Krishnasamy, S., Kumar, M.H., Parameswaranpillai, J., Rangappa, S.M. & Siengchin, S., *Interfacial Bonding Characteristics in Natural Fiber Reinforced Polymer Composites: Fiber-Matrix Interface In Biocomposites*, Springer: Singapore, pp.1–22, 2024.
[9] You, Y.J., Kim, J.H.J., Kim, S.J. & Park, Y.H., Methods to enhance the guaranteed tensile strength of GFRP rebar to 900 MPa with general fiber volume fraction. *Construction and Building Materials*, **75**, pp. 54–62, 2015.
[10] Sari, N.H., Sari, S., Sutaryono, Y.A. & Khan, M.A., A review: Fracture structure of natural fiber after treatment with various alkali chemicals. *Journal of Fibers and Polymer Composites*, **3**(2), pp. 158–180, 2024.
[11] Islam, T., Chaion, M.H., Jalil, M.A., Rafi, A.S., Mushtari, F., Dhar, A.K. & Hossain, S., Advancements and challenges in natural fiber-reinforced hybrid composites: A comprehensive review. *SPE Polymers*, **5**(4), pp. 481–506, 2024.
[12] Mohammed, M., Mohammed, A.M., Oleiwi, J.K., Adam, T., Betar, B.O., Gopinath, S.C.B., Ihmedee, F.H. & Anton, K., Influence of fiber treatments on water absorption behavior in natural fiber-reinforced polymer composites: A review. *Al-Rafidain Journal of Engineering Sciences*, **3**(1), pp. 410–430, 2025.
[13] Du, K., Zhang, D., Zhang, S. & Tam, K.C., Advanced functionalized materials based on layer-by-layer assembled natural cellulose nanofiber for electrodes: A review. *Small*, **20**, 2304739, 2024.
[14] Sarr, M.M. & Kosaka, T., Effect of cellulose nanofibers on the fracture toughness mode II of glass fiber/epoxy composite laminates. *Heliyon*, **9**(2), e13203, 2023.
[15] Wu, D., Xing, Y., Liu, L., Dong, Q., Wang, M. & Zhang, R., Structural design of 'straw and clay' based on cellulose nanofiber/polydopamine and its interfacial stress dissipation mechanisms. *International Journal of Biological Macromolecules*, **283**(4), 138040, 2024.
[16] Mathurosemontri, S., Auwongsuwan, P., Nagai, S. & Hamada, H., The effect of injection speed on morphology and mechanical properties of polyoxymethylene/poly (lactic acid) blends. *Energy Procedia*, **56**, pp. 57–64, 2014.